Available online at www.sciencedirect.com
SciVerse ScienceDirect
Nuclear Physics A 914 (2013) 119–129
NUCLEAR PHYSICS A
www.elsevier.com/locate/nuclphysa

The first observation of the neutron-rich hypernucleus ${}^{6}_{\Lambda}\mathrm{H}$

Elena Botta

INFN Sezione di Torino and Università di Torino, Dipartimento di Fisica, via P. Giuria 1, Torino, Italy

Received 30 November 2012; received in revised form 5 February 2013; accepted 5 February 2013
Available online 8 February 2013

Abstract

The FINUDA experiment at DAΦNE, Frascati, has observed the neutron-rich hypernucleus ${}^{6}_{\Lambda}\mathrm{H}$ by searching for (π^+, π^-) pairs in coincidence from the $K^-_{stop} + {}^{6}\mathrm{Li} \to {}^{6}_{\Lambda}\mathrm{H} + \pi^+$ production reaction and the ${}^{6}_{\Lambda}\mathrm{H} \to {}^{6}\mathrm{He} + \pi^-$ mesonic weak decay. The production rate of ${}^{6}_{\Lambda}\mathrm{H}$ undergoing this two-body decay has been found to be $(2.9 \pm 2.0) \cdot 10^{-6}/K^-_{stop}$. The binding energy of ${}^{6}_{\Lambda}\mathrm{H}$ has been evaluated to be $B_\Lambda({}^{6}_{\Lambda}\mathrm{H}) = (4.0 \pm 1.1)$ MeV with respect to ${}^{5}\mathrm{H} + \Lambda$, jointly from production and decay.

A similar investigation has been carried out for the observation of the neutron-rich hypernucleus ${}^{9}_{\Lambda}\mathrm{He}$ by looking for the $K^-_{stop} + {}^{9}\mathrm{Be} \to {}^{9}_{\Lambda}\mathrm{He} + \pi^+$ reaction in coincidence with the ${}^{9}_{\Lambda}\mathrm{He} \to {}^{9}\mathrm{Li} + \pi^-$ mesonic weak decay; an upper limit for the production rate of ${}^{9}_{\Lambda}\mathrm{He}$ undergoing the two-body decay has been found to be $4.2 \cdot 10^{-6}/K^-_{stop}$ (90% C.L.).

Keywords: Hypernuclei; Kaon-induced reactions; Nucleon distributions and halo features

1. Introduction

When a Λ hyperon is bound in a nucleus, its strangeness content prevents the effect of the Pauli exclusion principle, allowing the hyperon to populate deep Single Particle Shell Model states. In s- and p-shell hypernuclei particle-stable states are formed mostly with the Λ in the $1s$-shell; consequently, the total binding energy of the system is (often) considerably increased with respect to the core nucleus and also unstable nuclear cores can be bound and form stable

E-mail address: botta@to.infn.it.

0375-9474/$ – see front matter
http://dx.doi.org/10.1016/j.nuclphysa.2013.02.007

hypernuclei. The rôle of the Λ hyperon in stabilizing nuclear cores was first pointed out in the early 60s by Dalitz and Levi Setti [1] in a discussion concerning the existence of light hypernuclei with large neutron excess; the starting point was the observation of ${}^{6}_{\Lambda}$He, ${}^{7}_{\Lambda}$Be, ${}^{8}_{\Lambda}$He, ${}^{9}_{\Lambda}$Be and ${}^{10}_{\Lambda}$B hypernuclei in emulsion experiments [2], corresponding to unbound core systems.

No unstable-core hydrogen Λ hypernuclei have been found so far, although the existence of the lightest possible one ${}^{6}_{\Lambda}$H was predicted in [1] and subsequently reinforced in estimates by Majling [3]. More recently, Akaishi et al. [4] have evaluated the binding energy for ${}^{6}_{\Lambda}$H in a framework based on a coherent ΛN–ΣN mixing process, following a model originally developed for reproducing the binding energies of ${}^{4}_{\Lambda}$H, ${}^{4}_{\Lambda}$He and ${}^{5}_{\Lambda}$He [5]. The neutral-baryon excess in ${}^{6}_{\Lambda}$H, in particular, would be $(N+Y)/Z = 5$, with $Y = 1$ for a Λ hyperon, or $N/Z = 4$, larger than the maximal value in light nuclei, $N/Z = 3$ for ^{8}He [6]. Neutron-rich light hypernuclei could thus go beyond the neutron drip line for ordinary nuclear systems. The study of ${}^{6}_{\Lambda}$H and of heavier neutron-rich hypernuclei could place valuable constraints on the size of coherent ΛN–ΣN mixing also in dense strange neutron-rich matter [4]. This mixing provides a robust mechanism for generating three-body ΛNN interactions, with immediate impact on the stiffness/softness of the equation of state for hyperons in neutron-star matter [7] and on both the maximum mass achievable for neutron-stars and their mass–radius relation.

Neutron-rich hypernuclei could be produced by the two-body double charge-exchange reactions:

$$K^- + {}^{A}Z \to {}^{A}_{\Lambda}(Z-2) + \pi^+, \tag{1}$$

induced on nuclear targets by stopped or in flight K^- mesons, and

$$\pi^- + {}^{A}Z \to {}^{A}_{\Lambda}(Z-2) + K^+ \tag{2}$$

with π^- mesons in flight ($p_{\pi^-} > 0.89$ GeV$/c$).

These reactions can be described as two-step processes involving two different protons of the same nucleus and converting them into a Λ and a neutron, with the additional condition that the final nuclear system is bound. Another mechanism could be a single-step double charge exchange $m_i^- p \to \Sigma^- m_f^+$ (where m_i stands for the initial π^-/K^- and m_f for the final K^+/π^+) feeding the Σ component coherently admixed into the final Λ-hypernuclear state. The two-step processes are expected to occur at a rate $\leqslant 10^{-2}$ smaller [8] than the production of normal Λ hypernuclei by means of the corresponding single-step two-body reactions (K^-, π^-) and (π^+, K^+).

The first experimental attempt to produce neutron-rich hypernuclei was carried out at KEK [9] with the reaction (1) with K^- at rest. Upper limits were obtained for the production of ${}^{9}_{\Lambda}$He, ${}^{12}_{\Lambda}$Be and ${}^{16}_{\Lambda}$C hypernuclei (on ^{9}Be, ^{12}C and ^{16}O targets respectively) in the range of $(0.6\text{–}2.0) \cdot 10^{-4}/K^-_{\rm stop}$. Another KEK experiment [10] reported the production of ${}^{10}_{\Lambda}$Li in the (π^-, K^+) reaction on a ^{10}B target using a 1.2 GeV$/c$ π^- beam, with a cross section of 11.3 ± 1.9 nb/sr integrated over the Λ-bound region. However, no distinct bound-state structure could be resolved.

A further attempt to observe neutron-rich hypernuclei by means of the reaction (1) with K^- at rest was made at the DAΦNE collider at LNF by the FINUDA experiment [11], on ^{6}Li and ^{7}Li targets. From the analysis of a partial data sample, upper limits were evaluated for Λ-hypernuclear production: $R_{\pi^+}({}^{6}_{\Lambda}{\rm H}) < (2.5 \pm 0.4_{\rm stat}{}^{+0.4}_{-0.1\,{\rm syst}}) \cdot 10^{-5}/K^-_{\rm stop}$, $R_{\pi^+}({}^{7}_{\Lambda}{\rm H}) < (4.5 \pm 0.9_{\rm stat}{}^{+0.4}_{-0.1\,{\rm syst}}) \cdot 10^{-5}/K^-_{\rm stop}$. In addition an upper limit was estimated for ${}^{12}_{\Lambda}$Be: $R_{\pi^+}({}^{12}_{\Lambda}{\rm Be}) < (2.0 \pm 0.4_{\rm stat}{}^{+0.3}_{-0.1\,{\rm syst}}) \cdot 10^{-5}/K^-_{\rm stop}$, which lowers by a factor $\sim$3 the previous KEK determination [9].

Recently, analyzing the complete available data sample, the FINUDA experiment has reported the experimental evidence for the existence of ${}^{6}_{\Lambda}\mathrm{H}$ [12,13]. The increased statistics has been exploited to reduce the overwhelming background events in reaction (1) with K^- at rest by requiring a coincidence with π^- from the two-body weak decay of the produced hypernucleus:

$$K^-_{\mathrm{stop}} + {}^{6}\mathrm{Li} \to {}^{6}_{\Lambda}\mathrm{H} + \pi^+ \quad (p_{\pi^+} \sim 252\ \mathrm{MeV}/c), \tag{3}$$

$${}^{6}_{\Lambda}\mathrm{H} \to {}^{6}\mathrm{He} + \pi^- \quad (p_{\pi^-} \sim 134\ \mathrm{MeV}/c). \tag{4}$$

The same method has also been applied to the search of ${}^{9}_{\Lambda}\mathrm{He}$ produced on ${}^{9}\mathrm{Be}$ targets. In this paper a description of the coincidence technique is given and results on production rates are discussed.

2. Method for observation of ${}^{6}_{\Lambda}\mathrm{H}$

FINUDA was a hypernuclear physics experiment installed at one of the two interaction regions of the DAΦNE e^+e^- collider, the INFN-LNF $\Phi(1020)$-factory; a description of the experimental apparatus can be found in Ref. [13]. Only experimental features relevant to the present analysis are briefly recalled here. For π^+ with momentum ∼250 MeV/c the resolution of the tracker is $\sigma_p = (1.1 \pm 0.1)$ MeV/c [14] and the precision on the absolute momentum calibration is better than 0.12 MeV/c for the ${}^{6}\mathrm{Li}$ targets. For π^- with momentum ∼130 MeV/c the resolution and absolute calibration precision are respectively $\sigma_p = (1.2 \pm 0.1)$ MeV/c and 0.2 MeV/c.

Because the stopping time of ${}^{6}_{\Lambda}\mathrm{H}$ in metallic Li is shorter than its lifetime, both production (3) and decay (4) occur mainly at rest. For (3) it can be written explicitly:

$$M\left(K^-\right) + 3M(p) + 3M(n) - B\left({}^{6}\mathrm{Li}\right) = M\left({}^{6}_{\Lambda}\mathrm{H}\right) + T\left({}^{6}_{\Lambda}\mathrm{H}\right) + M\left(\pi^+\right) + T\left(\pi^+\right), \tag{5}$$

in which, in obvious notation, M stands for a particle mass, T for its kinetic energy, and $B({}^{6}\mathrm{Li})$ indicates the binding energy of ${}^{6}\mathrm{Li}$. For (4) it can be written:

$$M\left({}^{6}_{\Lambda}\mathrm{H}\right) = 2M(p) + 4M(n) - B\left({}^{6}\mathrm{He}\right) + T\left({}^{6}\mathrm{He}\right) + M\left(\pi^-\right) + T\left(\pi^-\right), \tag{6}$$

in the same notation as above. A straightforward algebra leads to the following expression for $T_{\mathrm{sum}} \equiv T(\pi^+) + T(\pi^-)$:

$$T_{\mathrm{sum}} = M\left(K^-\right) + M(p) - M(n) - 2M(\pi) - B\left({}^{6}\mathrm{Li}\right) + B\left({}^{6}\mathrm{He}\right) - T\left({}^{6}\mathrm{He}\right) - T\left({}^{6}_{\Lambda}\mathrm{H}\right). \tag{7}$$

The value of T_{sum} varies merely by 50 keV upon varying $B_\Lambda({}^{6}_{\Lambda}\mathrm{H})$ by 1 MeV, therefore negligibly with respect to the experimental energy resolution for a (π^+, π^-) pair in coincidence, $\sigma_T = 1.28$ MeV. Evaluating the r.h.s. of Eq. (7) by assuming $B_\Lambda({}^{6}_{\Lambda}\mathrm{H}) = 5$ MeV, from the average of 4.2 and 5.8 MeV predicted in Refs. [1,4], one obtains $T_{\mathrm{sum}} = 203 \pm 1.3$ MeV for ${}^{6}_{\Lambda}\mathrm{H}$ candidate events.

In the analysis events in the interval $T_{\mathrm{sum}} = 203 \pm 1$ MeV were considered, looking for a compromise between the contamination from background reactions discussed in more detail below, and the available statistics.

Fig. 1(left) shows a two-dimensional plot in the (p_{π^-}, p_{π^+}) plane for coincidence events selected in the band $T_{\mathrm{sum}} = 202$–204 MeV. The distribution drops above $p_{\pi^+} \simeq 245$ MeV/c and below $p_{\pi^-} \simeq 145$ MeV/c. This is close to the region where ${}^{6}_{\Lambda}\mathrm{H}$ events are expected. To search for particle-stable ${}^{6}_{\Lambda}\mathrm{H}$ events below its $({}^{4}_{\Lambda}\mathrm{H} + 2n)$ lowest threshold (see Fig. 2), using the two-body kinematics of Eqs. (3) and (4), a further requirement of $p_{\pi^+} > 251.9$ MeV/c and $p_{\pi^-} <$

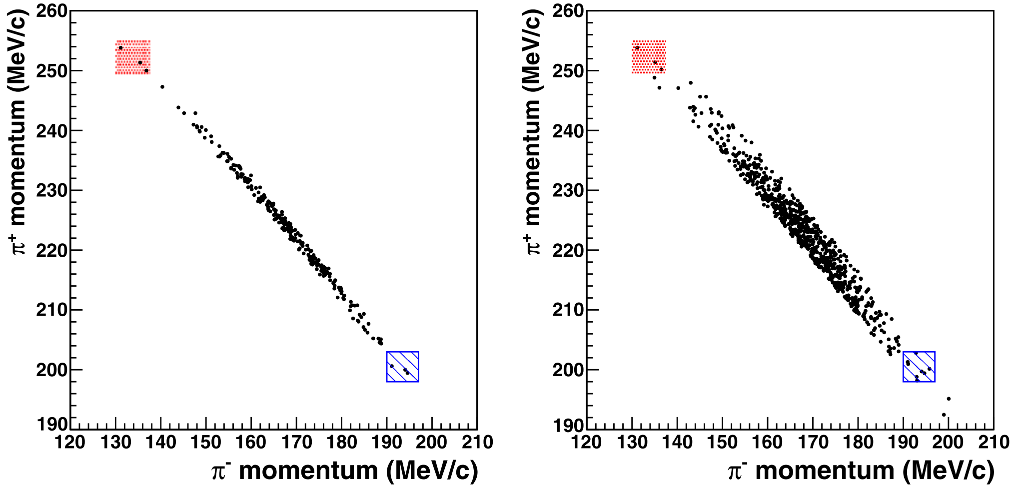

Fig. 1. (Color online.) π^+ momentum vs π^- momentum for ^{6}Li target events with $T(\pi^+) + T(\pi^-) = 202$–$204$ MeV (l.h.s.) and with $T(\pi^+) + T(\pi^-) = 200$–$206$ MeV (r.h.s.). The shaded (red) rectangles on each side consist of a subset of events with $p_{\pi^+} = 250$–255 MeV$/c$ and $p_{\pi^-} = 130$–137 MeV$/c$. The hatched (blue) rectangles on each plot are symmetric subsets of events to those in the shaded rectangles. From [13].

135.6 MeV$/c$ is necessary. The ranges $p_{\pi^+} = (250$–$255)$ MeV$/c$ and $p_{\pi^-} = (130$–$137)$ MeV$/c$ were selected, covering a $^6_\Lambda$H mass range from the $(\Lambda + {}^3\text{H} + 2n)$ threshold, about 2 MeV in the $^6_\Lambda$H continuum (see Fig. 2 for a scheme of particle emission thresholds), down to a $^6_\Lambda$H bound somewhat stronger than predicted by Akaishi et al. [4]. This does not completely exclude possible contributions from the production and decay of $(^4_\Lambda\text{H} + 2n)$. A complete discussion of the analysis technique can be found in [12,13].

3. $^6_\Lambda$H results

Out of a total number of $\sim 2.7 \cdot 10^7$ K^- stopped in the ^{6}Li targets, three events that satisfy the final requirements were found, as shown within the (red) shaded rectangle in Fig. 1(left). Different choices of $T(\pi^+) + T(\pi^-)$ interval widths (2–6 MeV) and position (center in 202–204 MeV) and of p_{π^+}/p_{π^-} interval widths (5–10 and 8–15 MeV$/c$) with fixed limits at 250 and 137 MeV$/c$ respectively to exclude the unbound region, affect the populations of the corresponding single spectra but not the coincidence spectrum. As an example, in Fig. 1 a comparison is made between the (p_{π^+}, p_{π^-}) plots satisfying the actual selection $T(\pi^+) + T(\pi^-) = 202$–$204$ MeV (l.h.s.), and similar plots admitting a wider selection range $T(\pi^+) + T(\pi^-) = 200$–$206$ MeV (r.h.s.). The global population increases for the wider cut, as expected, but the events that satisfy simultaneously also the separate selections imposed on p_{π^+} and p_{π^-} (shaded rectangles in the upper left part of the plots) remain the same. A similar stability is *not* observed in the opposite corner of the plots where five additional events appear on the right plot upon extending the cut. It is possible, moreover, to see directly from the two-dimensional plots that variations of the independent momentum selections do not produce any effect. Systematic errors due to the applied analysis selection are thus ruled out.

The three $^6_\Lambda$H candidate events are listed in Table 1 together with nuclear mass values derived separately from production (3) and from decay (4); the errors reported for each event are evalu-

Table 1
Summed kinetic energy T_{sum}, pion momenta $p_{\pi^\pm}$, and mass values inferred for the three ${}^6_\Lambda$H candidate events from production (3) and decay (4). From [12].

T_{sum} (MeV)	p_{π^+} (MeV/c)	p_{π^-} (MeV/c)	$M({}^6_\Lambda\mathrm{H})_{prod.}$ (MeV)	$M({}^6_\Lambda\mathrm{H})_{decay}$ (MeV)
202.6 ± 1.3	251.3 ± 1.1	135.1 ± 1.2	5802.33 ± 0.96	5801.41 ± 0.84
202.7 ± 1.3	250.1 ± 1.1	136.9 ± 1.2	5803.45 ± 0.96	5802.73 ± 0.84
202.1 ± 1.3	253.8 ± 1.1	131.2 ± 1.2	5799.97 ± 0.96	5798.66 ± 0.84

ated directly from the tracker resolution for π^+ and π^-. These mass values yield a mean value $M({}^6_\Lambda\mathrm{H}) = 5801.4 \pm 1.1$ MeV, jointly from production and decay, where the error is given by the spread of the average mass values for the three events.

Furthermore, we note from Table 1 that the mass values associated with production are systematically higher than those evaluated from the decay, by 0.98 ± 0.74 MeV. These mass differences could be connected to the excitation spectrum of ${}^6_\Lambda$H.

3.1. Background estimate, production rate evaluation and events discussion

A complete simulation of K^-_{stop} absorption reactions on single nucleons was performed, as well as on correlated two-nucleon clusters, that lead to the formation and decay of Λ and Σ hyperons. Full details can be found in [13], here it is sufficient to focus on one chain of reactions likely to produce (π^+, π^-) coincidences overlapping with those selected to satisfy ${}^6_\Lambda$H production (3) and decay (4): Σ^+ production, $K^-_{stop} + {}^6\mathrm{Li} \to \Sigma^+ + {}^4\mathrm{He} + n + \pi^-$, where $p_{\pi^-} \leqslant 190$ MeV/c, followed by Σ^+ decay in flight, $\Sigma^+ \to n + \pi^+$ ($p_{\pi^+} \leqslant 282$ MeV/c). The Σ^+ production was treated in the quasi-free approach, following the analysis of the FINUDA experiment observing $\Sigma^\pm\pi^\mp$ pairs [15]; in the signal region a small contribution of 0.16 ± 0.07 expected events was evaluated. The reaction chain of ${}^4_\Lambda$H hyperfragment production and two-body mesonic decay at rest ($p_{\pi^-} \sim 133$ MeV/c) has been estimated to deliver a negligible background of 0.04 ± 0.01 expected events. All other reaction chains that could produce (π^+, π^-) coincidences within the described selection ranges were ruled out by the applied selections. Turning to potential instrumental backgrounds, they could result from fake tracks, filtered because of reconstruction errors. To this end events coming from different nuclear targets used in the same runs (^{7}Li, ^{9}Be, ^{13}C, ^{16}O) were considered, with the same cuts. One event coming from ^{9}Be was found and accordingly 0.27 ± 0.27 expected fake events were evaluated from ^{6}Li, due to instrumental background.

A total background of 0.43 ± 0.28 expected events was evaluated. Thus, using Poisson distribution, the three ${}^6_\Lambda$H-assigned events do not arise from background to a confidence level of 99%.

Given the above background estimates, plus efficiency, target purity and cut estimates, it is possible to evaluate the product $R(\pi^+) \cdot \mathrm{BR}(\pi^-)$, where $R(\pi^+)$ is the ${}^6_\Lambda$H production rate per K^-_{stop} in reaction (3) and $\mathrm{BR}(\pi^-)$ the branching ratio for the two-body π^- decay (4):

$$R(\pi^+) \cdot \mathrm{BR}(\pi^-) = (2.9 \pm 2.0) \cdot 10^{-6}/K^-_{stop}. \tag{8}$$

Assuming $\mathrm{BR}(\pi^-) = 49\%$, as for the analogous ${}^4_\Lambda\mathrm{H} \to {}^4\mathrm{He} + \pi^-$ decay [16], it was found $R(\pi^+) = (5.9 \pm 4.0) \cdot 10^{-6}/K^-_{stop}$, fully consistent with the previous FINUDA upper limit [11]. This production rate $R(\pi^+)$ is two to three orders of magnitude smaller than summed Λ-bound production rates $R(\pi^-)$ of normal light Λ hypernuclei in the (K^-_{stop}, π^-) reaction [14].

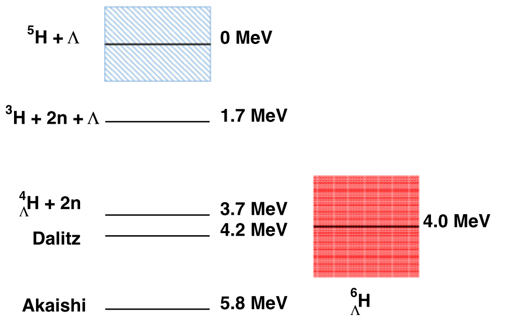

Fig. 2. $^{6}_{\Lambda}$H binding energy with respect to ^{5}H + Λ from three candidate events, as related to several particle emission thresholds and theoretical predictions. The location of ^{5}H with respect to the ^{3}H + 2n threshold (1.7 MeV below) is taken from [17]. From [13].

Table 1 yields a mean value $B_\Lambda(^{6}_{\Lambda}\mathrm{H}) = 4.0 \pm 1.1$ MeV with respect to ^{5}H + Λ, as shown in Fig. 2, in good agreement with the estimate 4.2 MeV [1] but considerably short of Akaishi's prediction $B^{\mathrm{th}}_\Lambda(^{6}_{\Lambda}\mathrm{H}) = 5.8$ MeV [4]. This indicates that coherent ΛN–ΣN mixing in the s-shell hypernucleus $^{4}_{\Lambda}$H [5] becomes rather ineffective for the excess p-shell neutrons in $^{6}_{\Lambda}$H.

The three events that give evidence for a particle-stable $^{6}_{\Lambda}$H can also give additional information on its excitation spectrum. It is expected to consist of a 0^+ g.s. and 1^+ excited state as in $^{4}_{\Lambda}$H (1.04 MeV), and a 2^+ excited state as for the p-shell dineutron system in ^{6}He (1.80 MeV). In fact, it is $^{6}_{\Lambda}\mathrm{H}(1^+)$ that is likely to be produced in reaction (3) simply because Pauli spin is conserved in production at rest, and the Pauli spin of ^{6}Li is $S = 1$ to better than 98%. The weak decay (4), however, occurs from $^{6}_{\Lambda}\mathrm{H}(0^+)$ g.s. since the (unseen) γ transition $1^+ \to 0^+$ is about three orders of magnitude faster than weak decay. Indeed, the production vs decay mass difference 0.98 ± 0.74 MeV extracted from the three $^{6}_{\Lambda}$H events listed in Table 1 is comparable to the underlying 1.04 MeV 1^+ excitation in $^{4}_{\Lambda}$H. In this case the B_Λ value for the g.s. would be larger $B_\Lambda(^{6}_{\Lambda}\mathrm{H}_{\mathrm{g.s.}}) = 4.5 \pm 1.2$ MeV. This scenario requires further experimental as well as theoretical inquiries.

4. Search for $^{9}_{\Lambda}$He

The neutron-rich hypernucleus $^{9}_{\Lambda}$He is one of the exotic Λ-hypernuclear species considered decades ago in [1] and by Majling [3] who estimated $B_\Lambda(^{9}_{\Lambda}\mathrm{He}) = 8.5$ MeV. Fig. 3 shows the expected g.s. $^{9}_{\Lambda}$He level, together with neutron emission thresholds below the 8.5 MeV Λ emission threshold.

Since ^{9}Be targets were used in the same data taking of FINUDA in which $^{6}_{\Lambda}$H was produced on ^{6}Li targets, with a similar number of stopped K^-, the possibility was examined whether the method applied to the successful search for $^{6}_{\Lambda}$H could be extended to the case of $^{9}_{\Lambda}$He. Results of this investigations have been published in [18].

$^{9}_{\Lambda}$He could be produced in the two-body reaction:

$$K^-_{\mathrm{stop}} + {}^{9}\mathrm{Be} \to {}^{9}_{\Lambda}\mathrm{He} + \pi^+. \tag{9}$$

Assuming $B_\Lambda(^{9}_{\Lambda}\mathrm{He}) = 8.5$ MeV, it is straightforward to evaluate the momentum $p_{\pi^+} = 257.5$ MeV/c for a π^+ meson emitted in (9). Since ^{9}Li g.s. is particle stable [19], admitting thus a two-body mesonic weak decay:

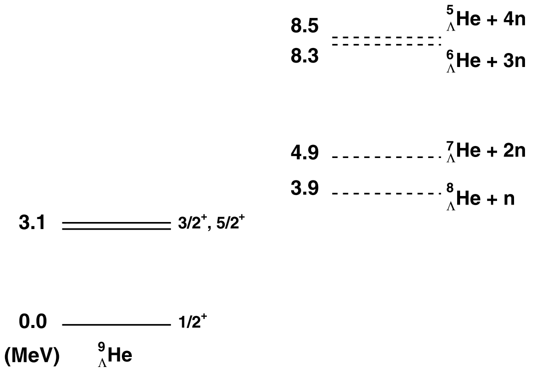

Fig. 3. ${}^{9}_{\Lambda}$He energy level scheme below the lowest neutron emission threshold, together with higher neutron emission thresholds. From [18].

$$ {}^{9}_{\Lambda}\mathrm{He}_{\mathrm{g.s.}} \to {}^{9}\Lambda\mathrm{Li}_{\mathrm{g.s.}} + \pi^- \tag{10}$$

that produces a π^- meson with $p_{\pi^-} = 116.9$ MeV$/c$, the coincidence method could indeed be applied. Observing that, also in this case, formation (9) and decay reaction (10) occur almost at rest, since the stopping time of ${}^{9}_{\Lambda}$He in the material (Be) is shorter than its lifetime (about 260 ps, the free-Λ lifetime), from momentum and energy conservation it is immediate to derive an equation analogous to (7):

$$T_{\mathrm{sum}} = M(K^-) + M(p) - M(n) - 2M(\pi) - B({}^{9}\mathrm{Be}) + B({}^{9}\mathrm{Li}) - T({}^{9}\mathrm{Li}) - T({}^{9}_{\Lambda}\mathrm{He}). \tag{11}$$

The value of T_{sum} varies by 10 keV upon varying $B_\Lambda({}^{6}_{\Lambda}\mathrm{H})$ by 1 MeV, negligible with respect to the experimental energy resolution discussed before. By considering a value of $B_\Lambda({}^{9}_{\Lambda}\mathrm{He}) = 8.5$ MeV [3], $T_{\mathrm{sum}} = 195.8 \pm 1.3$ MeV.

In this case, for the (π^+, π^-) coincidence only events for which T_{sum} assumed values in the range (194.5–197.5) MeV were considered. The two-dimensional plot of these selected events is shown in Fig. 4. Events associated with the formation of ${}^{9}_{\Lambda}$He with values of $B_\Lambda({}^{9}_{\Lambda}\mathrm{He})$ varying between 5 and 10 MeV should fall in the red rectangle in the figure, corresponding to $p_{\pi^+} =$ (253.5–259) MeV$/c$ and $p_{\pi^-} =$ (114.5–122) MeV$/c$. From Fig. 3 it is possible to see that a binding energy of 5 MeV is about 0.5 MeV below the lowest neutron emission threshold expected for ${}^{9}_{\Lambda}$He. There are clearly no events satisfying the conditions required by the formation and decay of ${}^{9}_{\Lambda}$He with $B_\Lambda({}^{9}_{\Lambda}\mathrm{He}) \geqslant 5$ MeV.

It was thus possible to derive an upper limit for ${}^{9}_{\Lambda}$He production rate $R(\pi^+) \cdot \mathrm{BR}(\pi^-)$, where $R(\pi^+)$ is the ${}^{9}_{\Lambda}$He production rate per stopped K^- in reaction (9) and $\mathrm{BR}(\pi^-)$ is the branching ratio (BR) for ${}^{9}_{\Lambda}$He two-body weak decay (10). Considering a 90% confidence level (C.L.), plus efficiency and cut estimates it was obtained:

$$\begin{aligned} R(\pi^+) \cdot \mathrm{BR}(\pi^-) &\leqslant \frac{N}{\epsilon(\pi^+)\epsilon(\pi^-)K^-_{\mathrm{stop}}({}^{9}\mathrm{Be})} \\ &= (2.3 \pm 1.9) \cdot 10^{-6}/K^-_{\mathrm{stop}} \to R(\pi^+) \cdot \mathrm{BR}(\pi^-) \\ &\leqslant 4.2 \cdot 10^{-6}/K^-_{\mathrm{stop}}. \end{aligned} \tag{12}$$

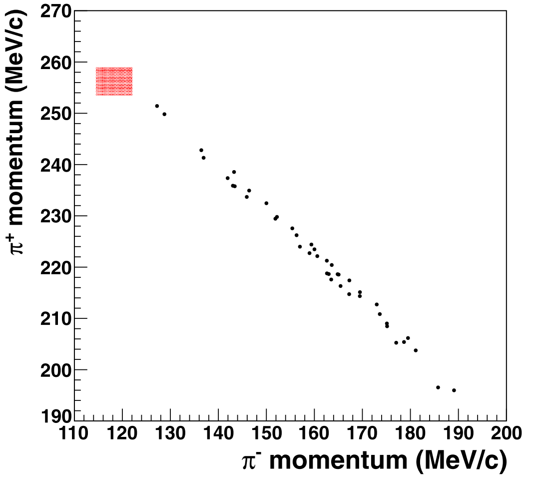

Fig. 4. (Color online.) π^+ momentum vs π^- momentum for ^{9}Be target events with $T_{sum} = 194.5$–197.5 MeV. The (red) shaded rectangle indicates the position of events with $p_{\pi^+} = 253.5$–259 MeV$/c$ and $p_{\pi^-} = 114.5$–122 MeV$/c$. From [18].

To derive the upper limit $R(\pi^+)$ for the production rate of $^9_\Lambda$He particle-stable levels, it is necessary to know the branching ratio BR(π^-) for the two-body weak decay $^9_\Lambda\mathrm{He}_{g.s.} \to {}^9\mathrm{Li}_{g.s.} + \pi^-$. In absence of published evaluations of the branching ratio for the weak decay $^9_\Lambda\mathrm{He}_{g.s.} \to {}^9\mathrm{Li}_{g.s.} + \pi^-$ in which a $1s$ Λ is transformed to a $1p$-proton, Ref. [20] was followed to evaluate $\Gamma({}^9_\Lambda\mathrm{He}_{g.s.} \to {}^9\mathrm{Li}_{g.s.} + \pi^-) = 0.261\ \Gamma_\Lambda$, where Γ_Λ is the free-Λ decay rate which approximates fairly the total Λ-hypernuclear decay rate in the relevant mass range [21]. Using the above BR(π^-) value, we obtain the following upper limit for the production of ^{9}He:

$$R(\pi^+) < (2.3 + 1.9)/0.261 \cdot 10^{-6}/K^-_{stop} = 1.6 \cdot 10^{-5}/K^-_{stop} \tag{13}$$

at 90% C.L. This improves by over an order of magnitude the previous upper limit set in the KEK experiment [9].

5. Production rates discussion and conclusions

Fig. 5 shows a synthesis of the present experimental knowledge on neutron-rich hypernuclei production rates with reaction (1) with K^- at rest. Shaded areas indicate upper limit values: red areas represent results for $^6_\Lambda$H, $^7_\Lambda$H and $^{12}_\Lambda$Be from [11], green areas represent results for $^9_\Lambda$He (out of scale), $^{12}_\Lambda$Be and $^{16}_\Lambda$C from [9], all obtained from inclusive π^+ spectra. Blue area and full circle represent the latest results on $^6_\Lambda$H and $^9_\Lambda$He from [12,13,18] derived with the (π^+, π^-) coincidence method.

Scarce theoretical calculations are available at present to compare with. In [22] the production of $^{12}_\Lambda$Be and $^{16}_\Lambda$C neutron rich hypernuclei has been studied in (K^-_{stop}, π^+) reaction; on top of a two-step process, a one-step production mechanism has been considered, $K^- p \to \pi^+ \Sigma^-$, proceeding through a small admixture of the virtual Σ^- component, which arises in Λ hypernuclei due to the ΛN–ΣN coupling, as a doorway state. An unusually eccentric Σ spatial distribution has been obtained and small admixture probabilities have been evaluated due to small overlap between halo and other baryons. The two-step double charge-exchange mechanism has turned

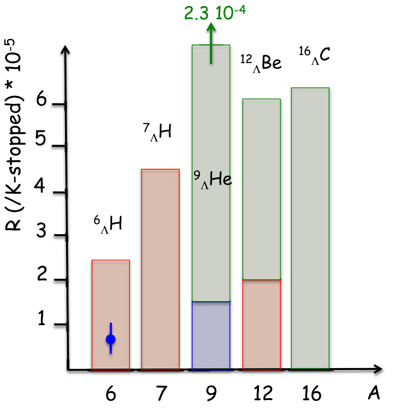

Fig. 5. (Color online.) Synopsis of the present experimental results on neutron-rich hypernuclei production rates with reaction (1) with K^- at rest. See text for more details.

out to be more productive. Quantitative predictions of production rates per stopped K^- lie in the interval $(10^{-6}–10^{-7})/K^-_{stop}$ and are at least one order of magnitude lower than the experimental upper limits from [9]. No calculation at all exists for the production rate of H and He neutron-rich hypernuclei. In this respect, it is desirable that FINUDA's recent results could stimulate detailed theoretical works.

From the experimental side it must be observed that the (π^+, π^-) coincidence method described in this paper is effectively simple but delicate and cannot be applied directly to the search of higher mass neutron-rich hypernuclei without careful considerations. First of all, the method is based on the possibility of considering two-body reactions for both production and mesonic decay of the hypernucleus. The production reaction is actually a two-body process proceeding both through one- and two-step mechanisms. The decay reaction satisfies the condition only if the daughter nucleus is stable against strong interaction, which is the case for ^{6}He in the decay of $^6_\Lambda$H and for ^{9}Li in the decay of $^9_\Lambda$He, but it is not, for example, for ^{7}He in the decay of $^7_\Lambda$H; indeed, FINUDA could not derive a precise estimation of its production rate even if it was able to give an upper limit by considering the π^+ inclusive spectra [11]. On the contrary, when increasing the target nucleus mass in the p-shell up to ^{16}O, the condition is always verified, but the corresponding mesonic decay branching ratio markedly decreases down to less than 10%. Moreover, the method allows one only to evaluate the product $R(\pi^+) \cdot \mathrm{BR}(\pi^-)$, between the hypernucleus production rate per K^-_{stop} and the branching ratio for the two-body charged mesonic decay. It is thus unavoidable to rely on previous experimental determinations or on theoretical evaluations of BR to obtain the production rate value $R(\pi^+)$.

Finally, the method allows to identify uniquely the production and decay of the neutron-rich hypernucleus only if it is produced and decays from the same energy level. It was applied to $^6_\Lambda$H, reactions (3) and (4), in the hypothesis that the hypernucleus mass is the same in both processes and its validity is due to the fact that the width of the selected $T(\pi^+) + T(\pi^-)$ interval (2 MeV) allows to include both production and decay pions within the experimental resolution, assuming the 1^+ state of $^6_\Lambda$H is excited only by ∼1 MeV with respect to the 0^+ ground state, as determined from the data. For $^9_\Lambda$He, on the other hand, the same method can only partially detect the production of $(3/2^+, 5/2^+)$ excited states at about 3.1 MeV from the $1/2^+$ ground state, since the $T(\pi^+) + T(\pi^-)$ selected interval width equals 3 MeV. However, it is not possible to enlarge the total kinetic energy selection to avoid an unacceptable increase of the background due to the Σ^+ production and decay reaction chain. This concern is expected to be increasingly important for higher A, where higher excitation energies are expected for possible production states and different excited states are available for the decay daughter nucleus. The mass difference between the production and decay levels can be accounted for, when reducing energy conservation equations equivalent to (5) and (6), only if the excitation energy spectrum in already known from experiment or theory.

An experiment to produce ${}^{6}_{\Lambda}$H and ${}^{9}_{\Lambda}$He via the (π^-, K^+) reaction on thick ^{6}Li and ^{9}Be targets at 1.2 GeV/c has been approved [23] to run at the J-PARC K1.8 beamline and is just starting the experimental activity. The expected energy resolution is 2.5 MeV FWHM, and the expected statistics about 1–2 orders of magnitude higher than previous KEK experiments [9, 10]. A missing mass spectroscopy technique will be used to identify the production of bound or slightly unbound states, the (π^-, K^+) reaction being almost background free in the Λ bound region if compared with the (K^-, π^+) one. Nevertheless, the lack of the coincidence with the π^- from the hypernucleus decay reaction could make it quite difficult to have a clear signature of the event, in particular for ${}^{6}_{\Lambda}$H, whose tiny signal is sitting on a tail of the Λ unbound region more sizeable than for ${}^{9}_{\Lambda}$He. Moreover, a higher energy resolution may be necessary to have a definite determination of the ${}^{6}_{\Lambda}$H excitation spectrum.

Acknowledgements

This work was partially supported in the framework of the EU FP7-INFRASTRUCTURES-2011-1 "HadronPhysics3 – Study of Strongly Interacting Matter", under the Grant Agreement No. 283286 (Working Package No. 6 – "SPHERE").

References

[1] R.H. Dalitz, R. Levi Setti, Nuovo Cimento 30 (1963) 489.
[2] M. Jurić, et al., Nucl. Phys. B 52 (1973) 1.
[3] L. Majling, Nucl. Phys. A 585 (1995) 211c.
[4] Y. Akaishi, T. Yamazaki, in: Frascati Physics Series, vol. XVI, 1999, p. 59;
S. Shinmura, K.S. Myint, T. Harada, Y. Akaishi, J. Phys. G 28 (2002) L1;
Y. Akaishi, K.S. Myint, AIP Conf. Proc. 1011 (2008) 277;
Y. Akaishi, Prog. Theor. Phys. Suppl. 186 (2010) 378.
[5] Y. Akaishi, T. Harada, S. Shinmura, K.S. Myint, Phys. Rev. Lett. 84 (2000) 3539.
[6] D.R. Tilley, et al., Nucl. Phys. A 745 (2004) 155.
[7] J. Schaffner-Bielich, Nucl. Phys. A 804 (2008) 309;
J. Schaffner-Bielich, Nucl. Phys. A 835 (2010) 279.
[8] R.E. Chrien, C.B. Dover, A. Gal, Czech. J. Phys. 42 (1992) 1089.
[9] K. Kubota, et al., Nucl. Phys. A 602 (1996) 327.
[10] P.K. Saha, et al., Phys. Rev. Lett. 94 (2005) 052502.
[11] M. Agnello, et al., Phys. Lett. B 640 (2006) 145.
[12] M. Agnello, et al., Phys. Rev. Lett. 108 (2012) 042501.
[13] M. Agnello, et al., Nucl. Phys. A 881 (2012) 269.
[14] M. Agnello, et al., Phys. Lett. B 698 (2011) 219.
[15] M. Agnello, et al., Phys. Lett. B 704 (2011) 474.
[16] H. Tamura, et al., Phys. Rev. C 40 (1989) R479.
[17] A.A. Korsheninnikov, et al., Phys. Rev. Lett. 87 (2001) 092501.
[18] M. Agnello, et al., Phys. Rev. C 86 (2012) 057301.
[19] See http://www.nndc.bnl.gov/ for nuclear data compilation.
[20] A. Gal, Nucl. Phys. A 828 (2009) 72.

[21] E. Botta, T. Bressani, G. Garbarino, Eur. Phys. J. A 48 (2012) 41.
[22] T.Yu. Tretyakova, D.E. Lanskoy, Nucl. Phys. A 691 (2001) 51.
[23] A. Sakaguchi, et al., Production of neutron-rich Λ-hypernuclei with the double charge-exchange reaction, Proposal P10 (revised) for Nuclear and Particle Physics Experiments at J-PARC, http://j-parc.jp/NuclPart/Proposal_e.html.